

## Probing the Active Site of Newly Predicted Stable Janus Scandium Dichalcogenides for Photocatalytic Water-splitting

Xiaoyong Yang <sup>a,b</sup>, Amitava Banerjee <sup>\*c</sup>, Rajeev Ahuja <sup>b,c</sup>

<sup>a</sup> State Key Laboratory of Environment-friendly Energy Materials, National Collaborative Innovation Center for Nuclear Waste and Environmental Safety, Southwest University of Science and Technology, Mianyang 621010, China

<sup>b</sup> Condensed Matter Theory Group, Materials Theory Division, Department of Physics and Astronomy, Uppsala University, Box 516, 75120 Uppsala, Sweden

<sup>c</sup> Applied Materials Physics, Department of Materials and Engineering, Royal Institute of Technology (KTH), S-100 44 Stockholm, Sweden

\* Corresponding author: amitava245@gmail.com

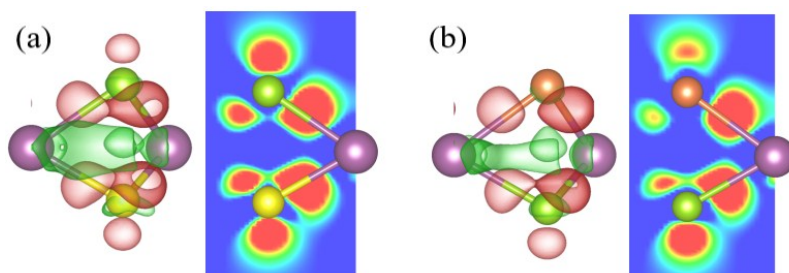


**Figure S1†** Isosurfaces of difference charge density for (a) ScSSe and (b) ScSeTe monolayers, respectively. The iso-surface is plotted at  $0.0055 e \text{ \AA}^{-3}$ . Red and green regions indicate accumulation and depletion of electrons, respectively.

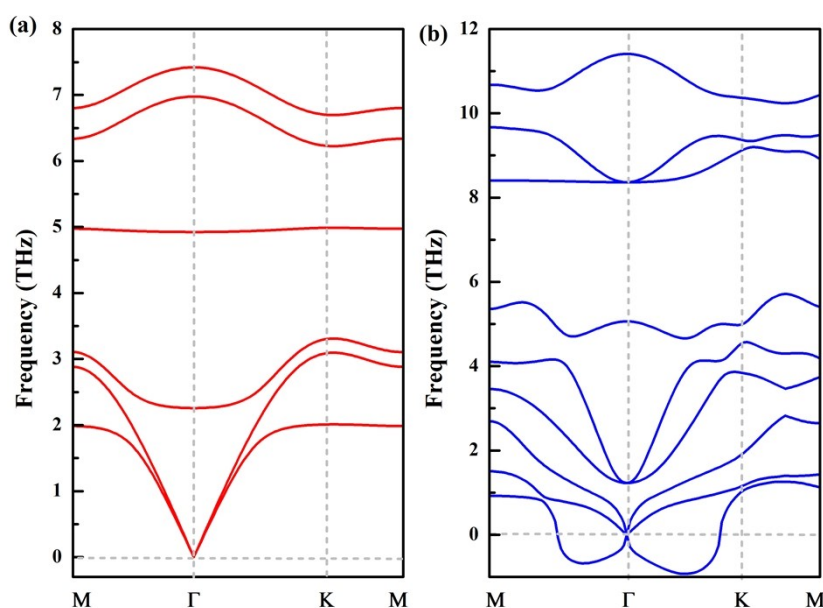


**Figure S2†** The calculated phonon dispersion curves for (a) ScSeTe and (b) ScSTe monolayers, respectively.

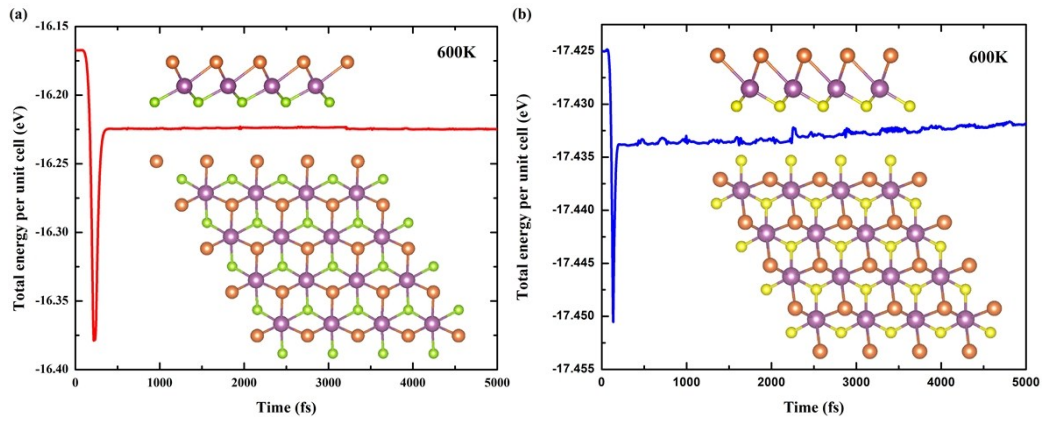


**Figure S3†** Variations of total energy of (a) ScSeTe and (b) ScSTe at 600 K during the time of 5 ps from AIMD simulation. Inset in (a) and (b) show the snapshots of the equilibrium structure from top and side views of ScSeTe and ScSTe monolayer at 600K, respectively.

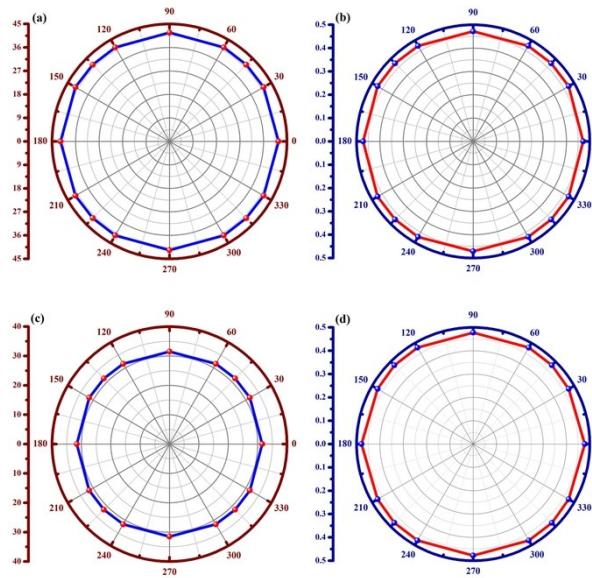


**Figure S4†** Young's modulus (a) (c) and Poisson's ratio (b) (d) of ScSSe and ScSeTe monolayers as a function of the angle  $\theta$ , respectively.

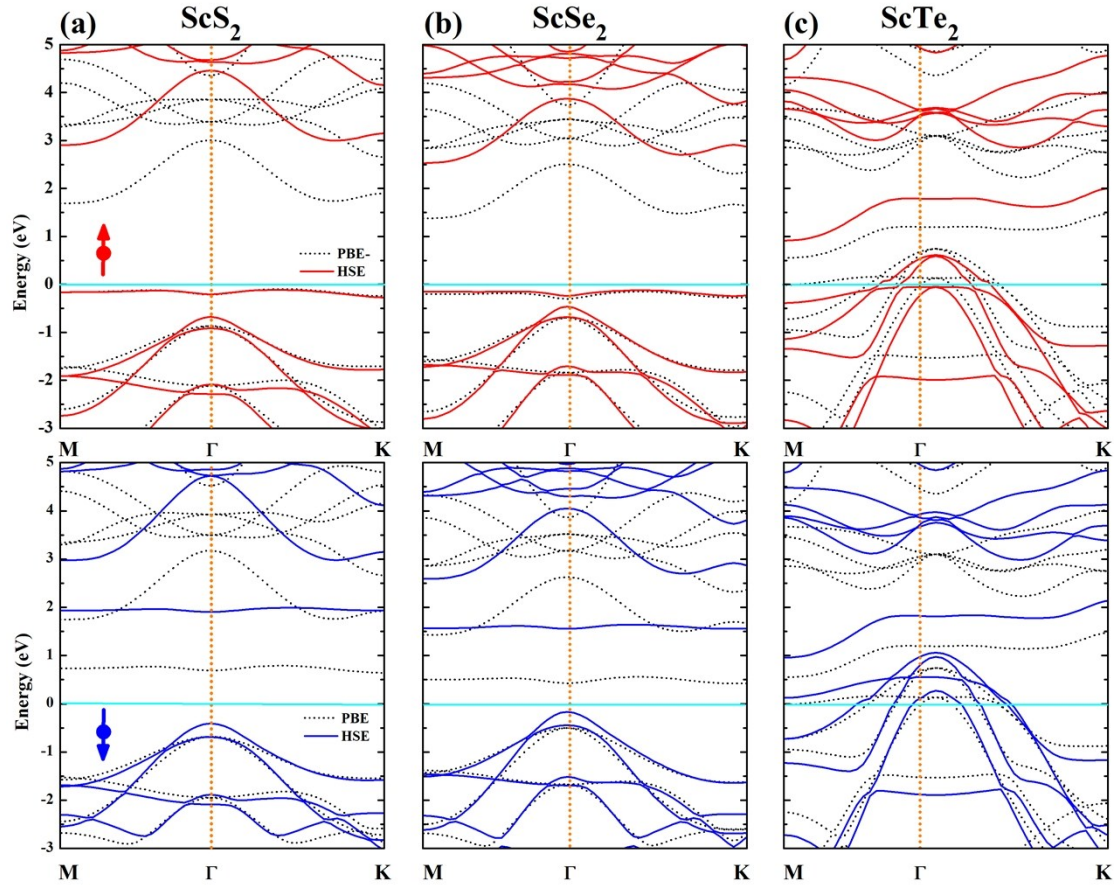


**Figure S5†** The electronic structures of (a)  $\text{ScS}_2$ , (b)  $\text{ScSe}_2$ , and (c)  $\text{ScTe}_2$  monolayers. The two rows indicate spin-up and spin-down, respectively. The solid and dash lines represent HSE06 and PBE calculations.

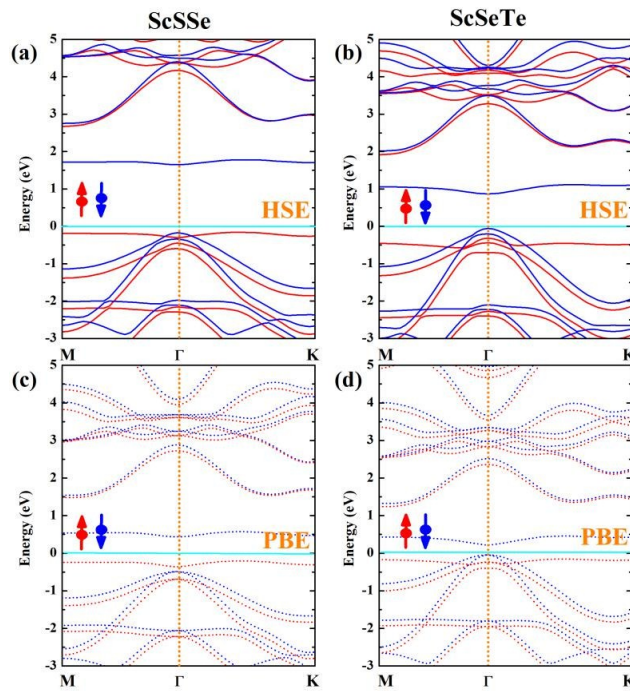


**Figure S6†** The electronic structures of (a) (c)  $\text{ScSSe}$  monolayer and (b)(d)  $\text{ScSeTe}$  monolayer from HSE06 (solid lines) and PBE (dash lines) functionals, respectively. Spin-up and spin-down bands are represented as red and blue lines, respectively.

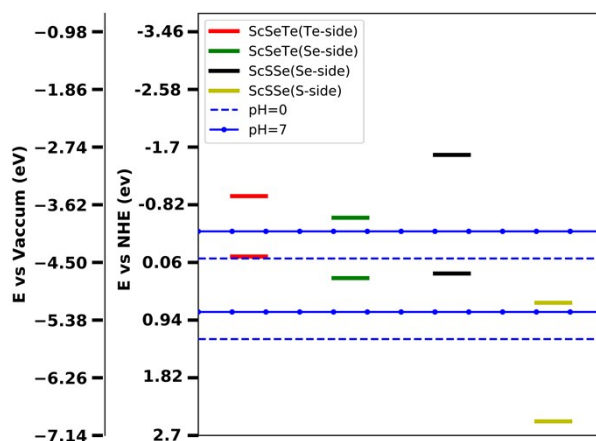


**Figure S7†** Band alignment with respective band edge of Janus layers, which is in contrast to our absorption free energy results. But edge specific alignment is consistent with the electronegativity of the chalcogenides and side specific electrostatic potential of Janus layers. It also agrees with the other Janus materials in the literature (J. Phys. Chem. C 2018, 122, 3123–3129). There exists a lot of materials in literatures (ACS Appl. Mater. Interfaces 2016, 8, 1536–1544, App. Phys. Lett., 2016, 109, 053903, Catal. Sci. Technol. 7, 687, 2017), that show good water splitting capability irrespective of the bandgap and band edge position. Therefore, in this article, we have focused on explicit interaction of the key intermediate of HER to predict good photocatalyst for water splitting.

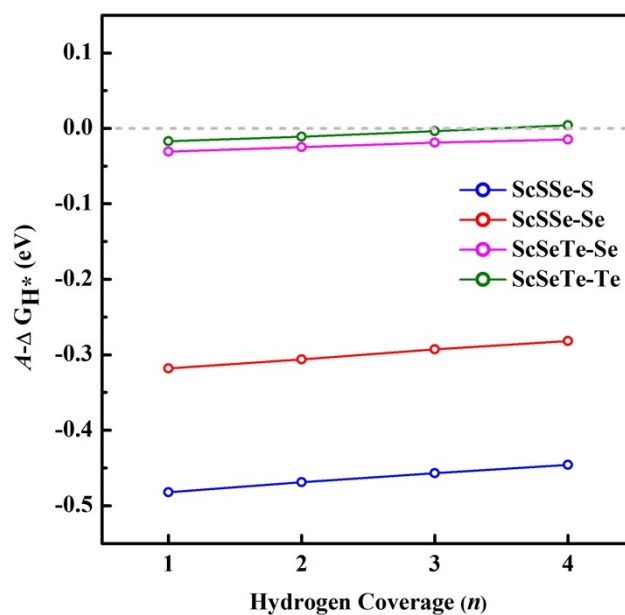


**Figure S8†** Hydrogen adsorption free energy diagram on the surfaces of Janus ScSSe and ScSeTe monolayers at different  $H^*$  coverages for average/collective process of HER.

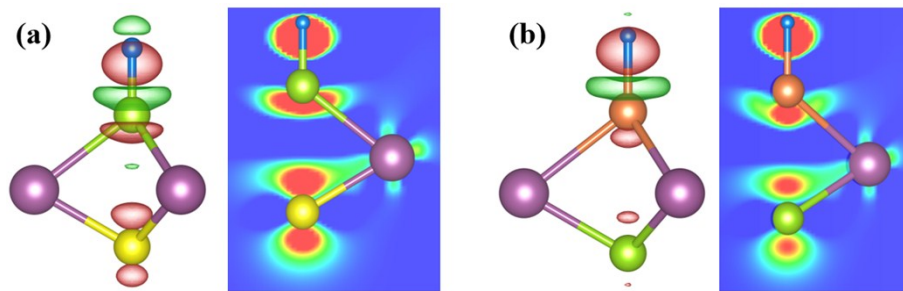


**Figure S9†** Isosurfaces of difference charge density for (a) pristine ScSSe and (b) ScSeTe monolayers with a H adatom, respectively. The iso-surface is plotted at  $0.0055 e \text{ \AA}^{-3}$ . Red and green regions indicate accumulation and depletion of electrons, respectively.

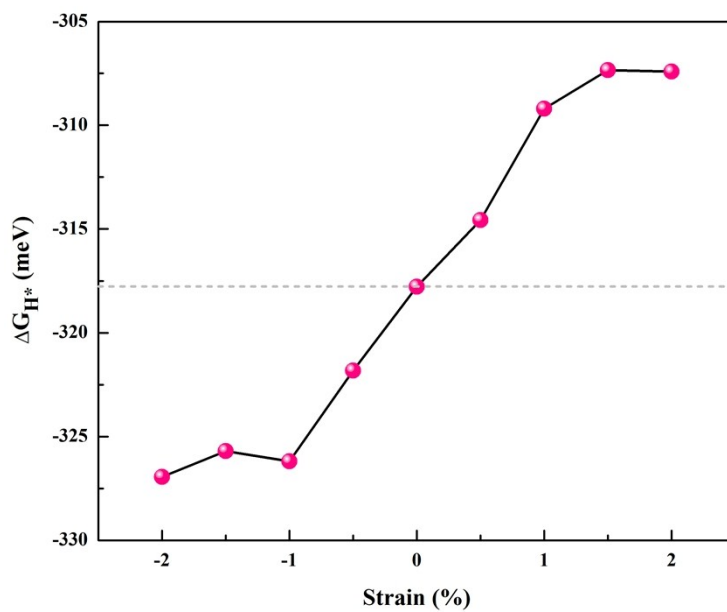


**Figure S10†** The calculated free energy of atomic hydrogen adsorption ( $\Delta G_{\text{H}^*}$ ) on the Se surface of Janus ScSSe monolayer as a function of strain.